A major purpose of the Technical Information Center is to provide the broadest dissemination possible of information contained in DOE's Research and Development Reports to business, industry, the academic community, and federal, state and local governments.

Although a small portion of this report is not reproducible, it is being made available to expedite the availability of information on the research discussed herein.

LA-UR--88-3613

DE89 002292

Los Alamos National Laboratory is operated by the University of California for the United States Department of Energy under contract W-7405-ENG-36

TITLE ONE DIMENSIONAL SIMULATION OF FREE-ELECTRON LASER OSCILLATOR USING A DIFFRACTION GRATING AS A CAVITY MIRROR

AUTHOR(S): H. Takeda, AT-6
J. E. Sollid, CLS-6

SUBMITTED TO Free Electron Laser Conf.,
Jerusalem, Israel, Aug. 29 - Sept. 2, 1988

DISCLAIMER

This report was prepared as an account of work sponsored by an agency of the United States Government. Neither the United States Government nor any agency thereof, nor any of their employees, makes any warranty, express or implied, or assumes any legal liability or responsibility for the accuracy, completeness, or usefulness of any information, apparatus, product, or process disclosed, or represents that its use would not infringe privately owned rights. Reference herein to any specific commercial product, process, or service by trade name, trademark, manufacturer, or otherwise does not necessarily constitute or imply its endorsement, recommendation, or favoring by the United States Government or any agency thereof. The views and opinions of authors expressed herein do not necessarily state or reflect those of the United States Government or any agency thereof.

By acceptance of this article, the publisher recognizes that the U.S. Government retains a nonexclusive, royalty-free license to publish or reproduce the published form of this contribution, or to allow others to do so, for U.S. Government purposes.

The Los Alamos National Laboratory requests that the publisher identify this article as work performed under the auspices of the U.S. Department of Energy

Los Alamos National Laboratory
Los Alamos, New Mexico 87545

MASTER

ONE-DIMENSIONAL SIMULATION OF A FREE-ELECTRON LASER OSCILLATOR USING A DIFFRACTION GRATING AS A CAVITY MIRROR*

H. Takeda and J. E. Sollid

Los Alamos National Laboratory, MS-E531, Los Alamos, NM 87545 USA

The free-electron laser (FEL) oscillator is known to excite parasitic sideband wavelengths in addition to the fundamental wavelengths at high intracavity power. When a tapered wiggler is used, the sidebands reduce the extraction efficiency. To eliminate the sidebands and to increase the extraction efficiency, we studied an FEL cavity with one of the mirrors ruled as a diffraction grating. The diffraction grating deflects the light in the cavity selectively according to the wavelength: the sidebands can be eliminated by deflection to off-axis of the cavity. Because the grating mirror must be mounted with an angle, laser pulse is stretched after diffraction. The pulse stretching reduces optical intensity. We studied the effect of pulse stretching numerically using a one-dimensional FEL code FELP.[1] Using this code, the free-electron laser performance is calculated and compared with different line densities of grating for the following three wigglers: an untapered wiggler, a 12% wavelength tapered wiggler, and a wiggler tapered in wave number by 30%. The wavelength aperture caused by the grating also is studied as a function of line density.

1. Introduction

To achieve a high extraction efficiency, the sidebands can be eliminated by several optical methods as discussed in ref. [1]. One of the methods utilizes the deflection of light in the cavity selectively according to the wavelength. This can be done by making one of the mirrors into a diffraction grating. Because the grating introduces stepwise discontinuities in the optical pulse, a rather high optical loss must be compromised with the merit of efficiency enhancement. The diffracted light pulse is also stretched temporally.

The effects of the grating on the optical pulse are three dimensional. To compare the optical results with the cavity without grating, in which sidebands are excited, we

* Work performed under the auspices of the U.S. Dept. of Energy and supported by the U.S. Army Strategic Defense Command.

[1] FELP is a one dimensional free electron laser code written by B.D. McVey, MS E531, Los Alamos National Laboratory, Los Alamos, NM 87545

have folded the three-dimensional effects induced by a grating into a one-dimensional, free-electron laser pulse code FELP. Using this code, the laser performance is calculated and compared for different line densities of grating.

Although the calculation performed here is idealized, similar gratings are built; a sideband suppression experiment was performed with an untapered wiggler at the Los Alamos free-electron laser facility as discussed in ref. [2].

2. The suppression of sidebands by a ruled mirror

Given a grating line spacing d, the incidence angle θ_i and the diffraction angle θ_u measured from the normal to the average surface are related by the grating formula as

$$\sin\theta_u = -\sin\theta_i + \frac{\lambda}{d} , \tag{1}$$

where λ is the wavelength of the laser.

When a grating is mounted to satisfy the Littrow condition, i.e., the incidence angle θ_i and the diffraction angle θ_u are set equal, they satisfy eq. (1) with $\theta_i = \theta_u$. By inspecting the geometry shown in fig. 1, we see that the grating blaze angle θ_{bl} is equal to θ_i. We designate the wavelength and the diffraction angle that satisfy the Littrow condition as λ_0 and θ_{u0} or θ_{i0}. Then, the grating formula reduces to

$$\sin\theta_{bl} = \sin\theta_{u0} = \sin\theta_{i0} = \frac{\lambda_0}{2d} . \tag{2}$$

Assuming that the grating is mounted at θ_{bl} for λ_0, and that a laser with a wavelength λ that differs from λ_0 shines on the grating with the angle of incidence at θ_{i0}, the diffraction angle θ_u is obtained as

$$\sin\theta_u = \frac{1}{2d}(2\lambda - \lambda_0) . \tag{3}$$

This equation shows that the sidebands, having wavelengths other than λ_0, are diffracted off axis. By canting the optical axis of the ruled mirror with the blaze angle θ_{bl} so that the Littrow ray with λ_0 stays on the cavity axis after successive diffraction, sidebands can be diffracted off axis of the cavity and eventually eliminated. Fig. 2 shows the cavity configuration.

The canted mirror modifies the ideal Gaussian mode in two ways: First, the light pulse is spectrally separated and is spread laterally. Second, the light pulse is stretched because the delay time of wavelets from lateral positions on the mirror is induced proportional to the distance from the center of the canted mirror.

Because any light pulse can be decomposed into wavelength components, we can explore the wavelength acceptance of the cavity by tracing a monochromatic ray in the cavity.

3. The wavelength acceptance of a cavity

When the pulse is stretched by the canted mirror and diffracted back to the cavity optical axis, the spectrum of the pulse narrows because the waves with the remaining wavelengths are diffracted to off-axis directions. When the wavelength is very different from λ_0, the cavity can not sustain these waves in subsequent passes and the waves at these wavelengths will be lost from the cavity.

Knowing the incidence angle θ_i and the incidence position at the mirror in the cavity, the diffracted ray can be calculated using eq. (1). By tracing the ray for a number of passes, the wavelength acceptance of the cavity can be obtained: The rays within the acceptance stay in the cavity, and the rays out of the acceptance are lost from the cavity. The ray with λ_0 traces on the cavity axis, but rays with other wavelengths bounce in the cavity with an angle to the optical axis and with a lateral displacement. Starting on-axis, a ray was traced up to 2000 passes. Table 1 shows the mirror and the cavity parameters used in the simulation. Apertures that correspond to three times the dimension's waists are imposed at the cavity center and at the mirrors to eliminate out-of-bound rays. A ray with a wavelength of 10.045 μm made only three round trips in the cavity and was then lost (fig. 3a). The number of hits at the ruled mirror is plotted as a function of lateral position at the mirror. When the wavelength of the ray is chosen closer to the Littrow wavelength $\lambda_0 = 10.1$ μm, the ray is contained in the cavity. At wavelength $\lambda = 10.084$ μm, the ray oscillated between the center of the mirror and the -0.9 cm position about the average position at -0.4 cm. The large entry at both ends shows that the intersection of the ray and the mirror moves slowly at both ends. At wavelength $\lambda = 10.124$ μm, the ray oscillates in a similar way, but the average position is at +0.5 cm. The ray with $\lambda = 10.143$ μm is lost after four passes, as seen in fig. 3c.

For gratings ruled with 6 lines/mm and 10 lines/mm, the wavelength acceptances $\delta\lambda/\lambda$ by ray tracing are obtained as 0.8% ± 0.1% and 0.4% ± 0.1%, respectively. If we neglect the transverse oscillation of rays at the mirror, the average ray position that corresponds to the intersection by a stationary ray in the cavity can be calculated analytically from geometrical considerations alone. This procedure yields acceptances about twice the ray

simulation.

4. The pulse stretching by a ruled mirror

We can assume that the optical cavity establishes approximately a Gaussian mode between mirrors. When an optical pulse exits from the undulator with its transverse Gaussian profile, the waist size r_0 is determined as a function of distance z from the center of the undulator as

$$r_0 = \sqrt{\frac{\lambda b}{2\pi}}\sqrt{1+\left(\frac{z}{b}\right)^2}\,, \tag{4}$$

where λ and b are the wavelength of the laser and the Rayleigh range. The pulse arrives at the ruled mirror after diffracting and expanding its waist while maintaining the Gaussian profile.

Satisfying the Littrow mounting condition, the optical axis of the mirror with grating is set to make an angle equal to the blaze angle θ_{bl} with respect to the cavity axis. One end of the Gaussian wing arrives at the mirror earlier than the other end of the wing. When the center of the pulse arrives at the center of the mirror, the wavefront from one end is already diffracted by the same distance as the distance from the wavefront of the other end to the mirror.

At the Littrow mounting, the first-order diffraction of light by the mirror emerges as if the light is reflectd by micromirrors mounted as stairs with spacing d and depth $1/2\lambda_0$ between them (fig. 4). When the wavelets from each micromirror are superposed along the direction of propagation, a stretching of the light pulse is observed. We are assuming that the mirror dimension is much smaller than the distance between the mirror and the wiggler so that diffraction arriving at the wiggler can be considered as Fraunhofer diffraction. Even if we assume that the light pulse that propagates to the mirror is on the optical axis of the cavity, the diffracted light from each micromirror is dispersed across the optical axis. Although the laterally dispersed pulse propagates to the mirror with grating at proceeding passes, only a pulse defined with the wavelengths surrounding the Littrow ray λ_0 remains in the cavity.

5. Simulations using a one-dimensional FELP code with pulse stretching

To fold the three dimensional diffraction effects into a one dimensional code, we make assumptions: 1. We assume that a diffracted light pulse has a narrow bandwidth as

determined from the spectral components of the stretched pulse. 2. We assume that each wavelet from the grating overlaps well with the electron beam at the wiggler.

The light pulse observed at the wiggler is the superposition of wavelets that are temporally displaced. At this superposition we impose weights from individual wavelet intensities. The light loss at the grating mirror is considered as a part of cavity loss because the material of the mirror and the ruling of the grating affect the amount of light diffracted into the first-order diffraction.

The parameters used in the simulation are shown in Table 2. Because the grating has a fixed, narrow bandwidth, the cant angle of the ruled mirror determines the center wavelength of the window. The cant angle must be set so that the gain at the center wavelength must far exceed the cavity loss. Because the gain curve changes its shape as the laser intensity increases, this condition must be satisfied simultaneously both at the small-signal and at the large-signal regime. The gain curves for the wiggler tapered parabolically by 30% in wave number are shown in fig. 5; the large signal gain is obtained with input intensity 1.7×10^{11} W/cm^2. We set the cant angle to give a wavelength of 10.25 μm; this is shown as the arrows in fig. 5. Similarly, the center wavelengths are set to 10.2 μm for other types of wigglers: the untapered wiggler and the 12% tapered wiggler. The center wavelengths are chosen as a compromise to obtain a large gain both at high intensity and at low intensity of the laser.

Calculating with the 30% wave number tapered wiggler, electric field profiles along the pulse are shown at the top row in fig. 6 for both the 6 lines/mm grating and the 10 lines/mm grating. After 300 passes, they are stretched significantly. The pulse profile for the unruled mirror shows a modulation caused by the sidebands. The Fourier transforms of the pulses are shown in the second row of fig. 6. When no grating is present, we observe a significant presence of sidebands.

Fig. 7 shows extraction efficiencies plotted with pass numbers for the 30% parabolically tapered wiggler; fig. 7a shows the 6 lines/mm grating, and fig. 7b shows the 10 lines/mm grating, showing peak current at 250 A and at 400 A. Although the gain curve of the 30% tapered wiggler is known to have a relatively small chirp in wavelength, it is more difficult to start up the system at low current for the mirror with 10 lines/mm grating because the pulse stretching reduces the peak intensity, and the effective gain seen by the system reduces. When there is no grating, the sidebands develop and the extraction efficiency fluctuates, as shown in fig. 8 at both electron beam currents. Also shown (fig. 8)

are the single-pass extraction efficiencies that correspond to the peak gain of 5.5%.

6. Effects of gratings with the three types of wiggler

Multipass simulations using the one-dimensional code FELP were performed up to 600 passes, where the efficiencies reached saturation. A uniform wiggler, a 12% tapered wiggler, and a 30% parabolically tapered wiggler are assumed for the simulations with two types of grating mirrors: a mirror ruled with 6 lines/mm, and a mirror ruled with 10 lines/mm.

The extraction efficiencies are plotted in fig. 9 as a function of electron-beam current for the untapered wiggler. For reference, the peak efficiencies of single-pass calculations are also plotted; the input powers are set so that the peak gain is about 5.5%. The optical power of the pulse reaches up to 0.5 GW and 2.0 GW with either grating at 250 A and at 400 A, respectively. Without gratings, the optical power of the pulse reaches up to 4.5 GW at 400 A. However, the extraction efficiencies with either grating are at least a factor of 2 lower than without gratings. This result shows that the pulse stretching by the grating reduces the extraction efficiency significantly. Comparing the efficiencies between no-grating and the single pass, we conclude that the sidebands contribute a higher extraction efficiency by over a factor of 2 at low current.

The extraction efficiencies for the 12% tapered wiggler are plotted in a manner similar to that for the untapered wiggler (fig. 10). The single-pass peak efficiencies are also plotted for reference. The optical powers of the pulse are 3 GW and 5 GW with currents at 250 and 400 A, respectively. Except at low current (150 A), the efficiencies do not depend on the current, and they are almost equal for either case. The gratings fail to improve the efficiency except at low current.

The extraction efficiencies for the 30% parabolically tapered wiggler are plotted in fig. 11. The single-pass peak efficiencies are also plotted as a reference. The optical powers of the pulse with 6 lines/mm grating at saturation are 5 GW and 9 GW with currents at 250 and 400 A, respectively. Without gratings, the optical powers are 3.5 GW and 6 GW at these currents, where both the optical power and the extraction efficiencies fluctuate about ± 0.5 GW. Clearly, the gratings enhance the extraction efficiencies by a factor of at least 1.2 for the 30% tapered wiggler.

Table 1. Mirror and cavity parameters

Spherical mirror radii R	353 cm
Mirror separation $2D$	691.8 cm
Littrow ray λ_0	10.1 μm
Waist σ_0 at cavity center	0.89 mm
Waist σ_1 at mirror	6.33 mm
Aperture at cavity center $\pm 3\sigma_0$	$\pm$2.67 mm
Aperture at mirrors $\pm 3\sigma_1$	$\pm$1.9 cm
Rayleigh range b	49 cm
Grating line spacing d	10 lines/mm,
	6 lines/mm

Table 2. One-dimensional simulation parameters

E-beam peak current	150 A, 250 A, 350 A
E-beam energy	21 MeV
E-beam $\frac{\delta\gamma}{\gamma}$	1%
E-beam emittance	1 π·mm·mrad
E-beam pulse	10 *ps* parabolic profile
Grating line density	6 lines/mm, 10 lines/mm
Wiggler length	100 cm
Wiggler taper	Uniform, 12% in wavelength,
	30% parabolically in wavenumber
Wiggler period	2.73 cm at the entrance
Net intensity loss/pass	5% (including grating loss)

References

[1] J. E. Sollid, D. W. Feldman, and R. W. Warren,"Sideband Suppression for the Los Alamos Free-Electron Laser," this conference.

[2] J. E. Sollid, D. W. Feldman, R. W. Warren, H. Takeda, S. Gitomer, J. Johnson, and W. Stein, "Sideband Suppression in the Los Alamos Free-Electron Laser using a Littrow Grating," this conference.

Figure captions

Figure 1. In a mirror mounted to satisfy the Littrow mounting condition, the incident angle θ_i, the diffraction angle θ_u, and the blaze angle θ_{bl} are equal.

Figure 2. A cavity with a mirror ruled with grating. The mirror is canted at blaze angle θ_{bl}. The optical mode is semi-Gaussian.

Figure 3. Distribution of ray positions at the ruled mirror. The number of rays that hit the mirror is shown as a function of position on the mirror. The wavelenth of the ray determines the average position.

Figure 4. The pulse-stretching mechanism. Rays see the Littrow-mounted mirror with grating as stairs with a height $\lambda_0/2$. Successive wavelets are displaced by λ_0, and the pulse is stretched after superposition.

Figure 5. Small-signal and large-signal gain curves for the 30% tapered wiggler. The cant angles of the ruled mirrors are set so that they correspond to 10.25 μm.

Figure 6. The stretched pulse profiles and the spectra are shown for gratings with 6 lines/mm, with 10 lines/mm, and without gratings. Each spectrum has a single line when gratings are used.

Figure 7. Extraction efficiencies with gratings for the 30% parabolically tapered wiggler.

Figure 8. Extraction efficiencies without gratings and efficiencies by single-pass calculation. The peak gain is set to 5.5% for the single-pass calculation.

Figure 9. The efficiencies for the untapered wiggler. The single-pass efficiencies are obtained for a peak gain of 5.5%, thereby showing that the sidebands enhance efficiency and that the grating reduces efficiency.

Figure 10. The efficiencies for the 12% tapered wiggler show that the grating is ineffective in increasing the efficiency.

Figure 11. The efficiencies for the 30% parabolically tapered wiggler show that the efficiencies can be enhanced by the grating.

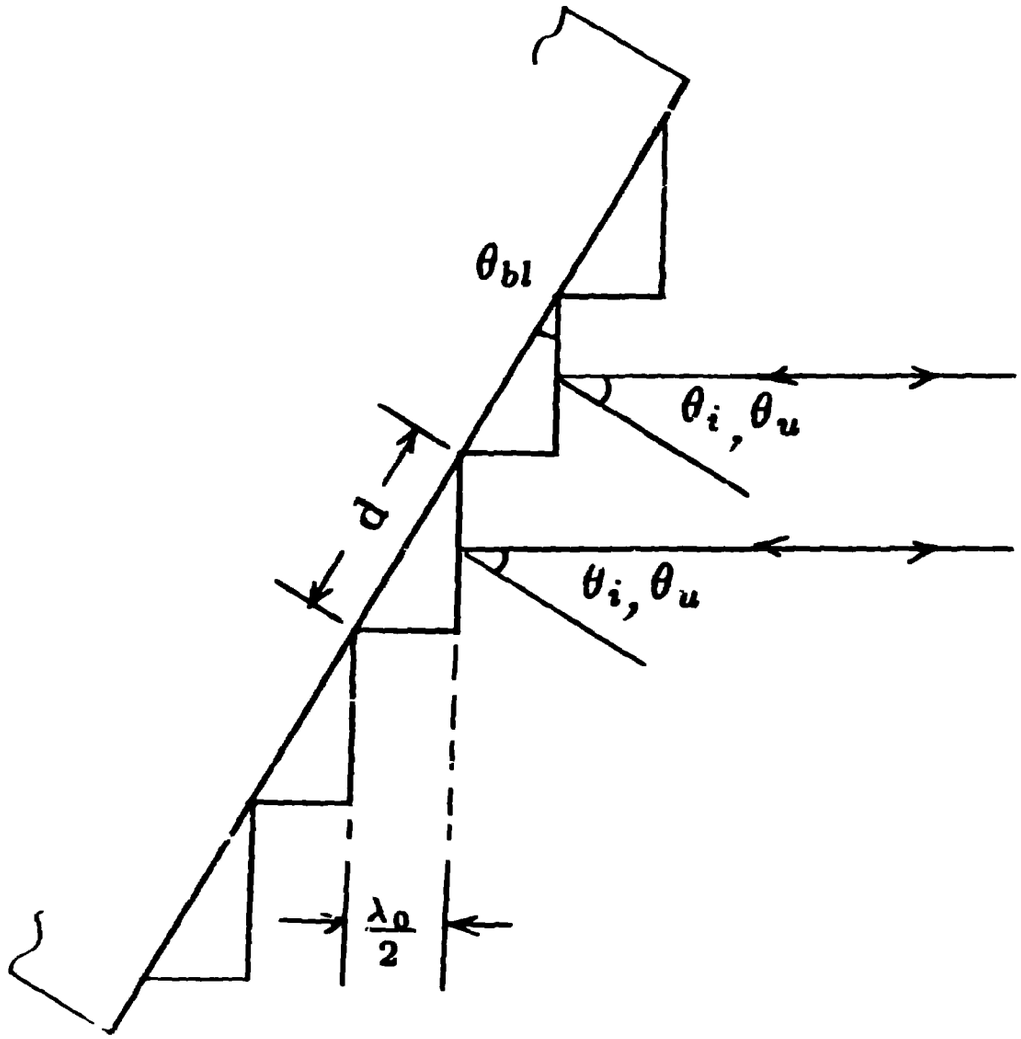
θ_{bl}
θ_i, θ_u
d
θ_i, θ_u
$\frac{\lambda_0}{2}$

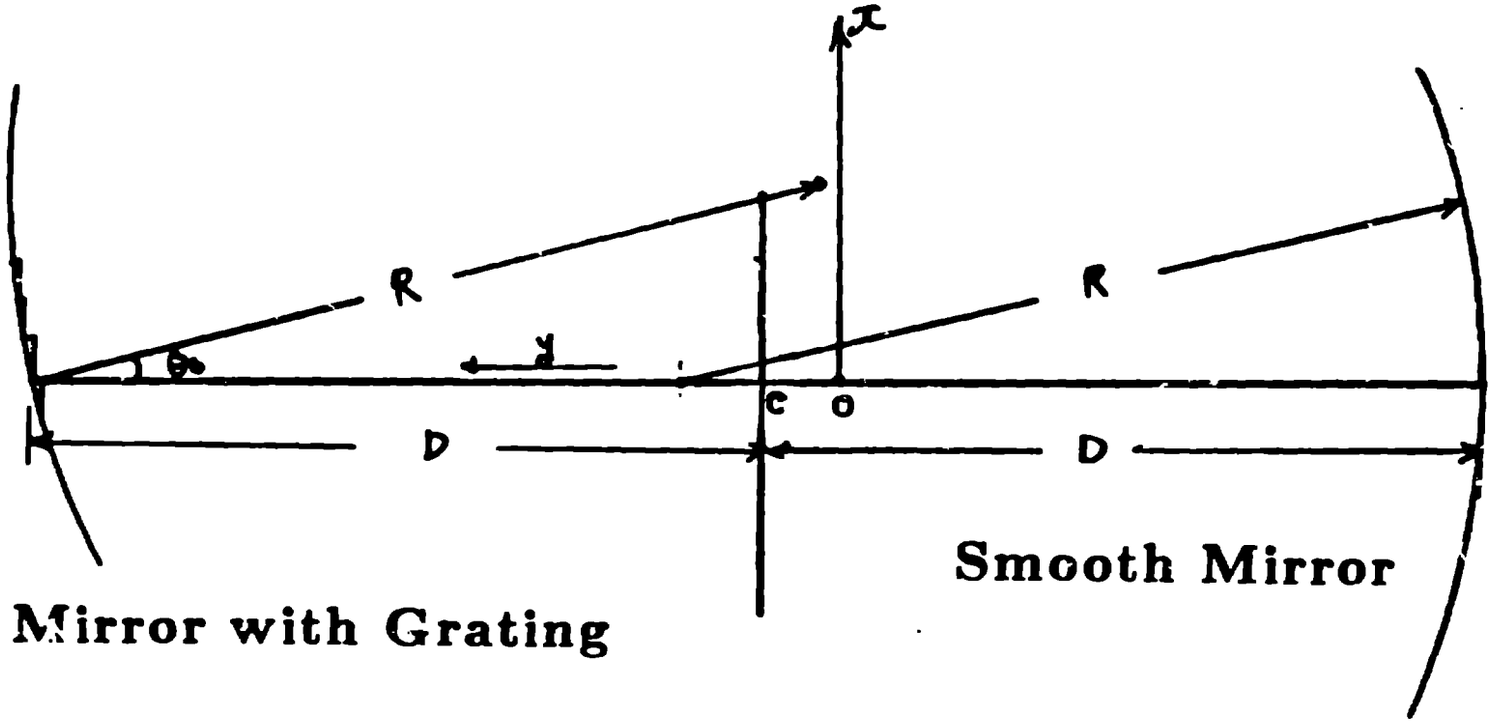
x
R
R
θ
y
C
O
D
D
Smooth Mirror
Mirror with Grating

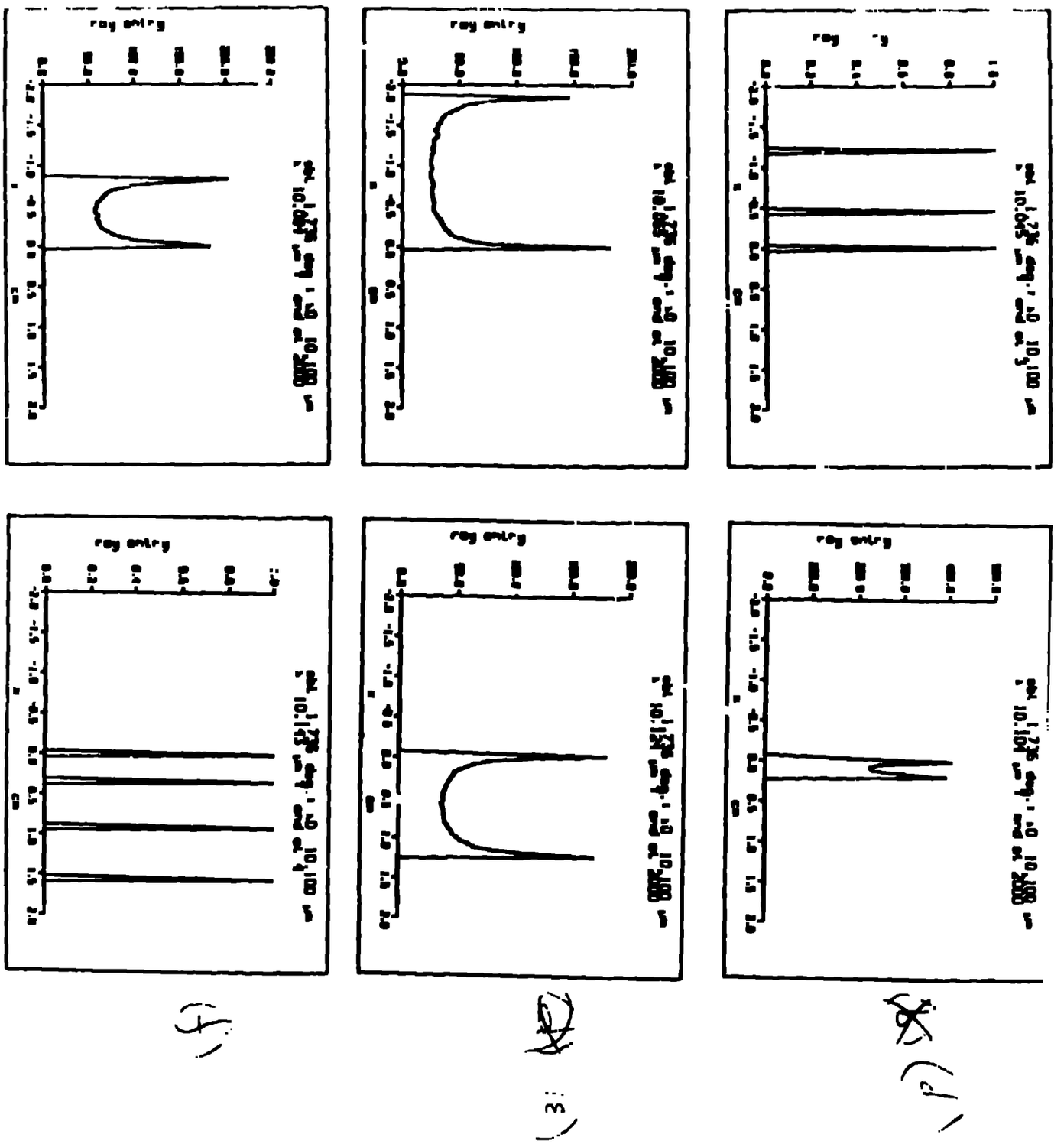

REPRODUCED FROM
BEST AVAILABLE COPY

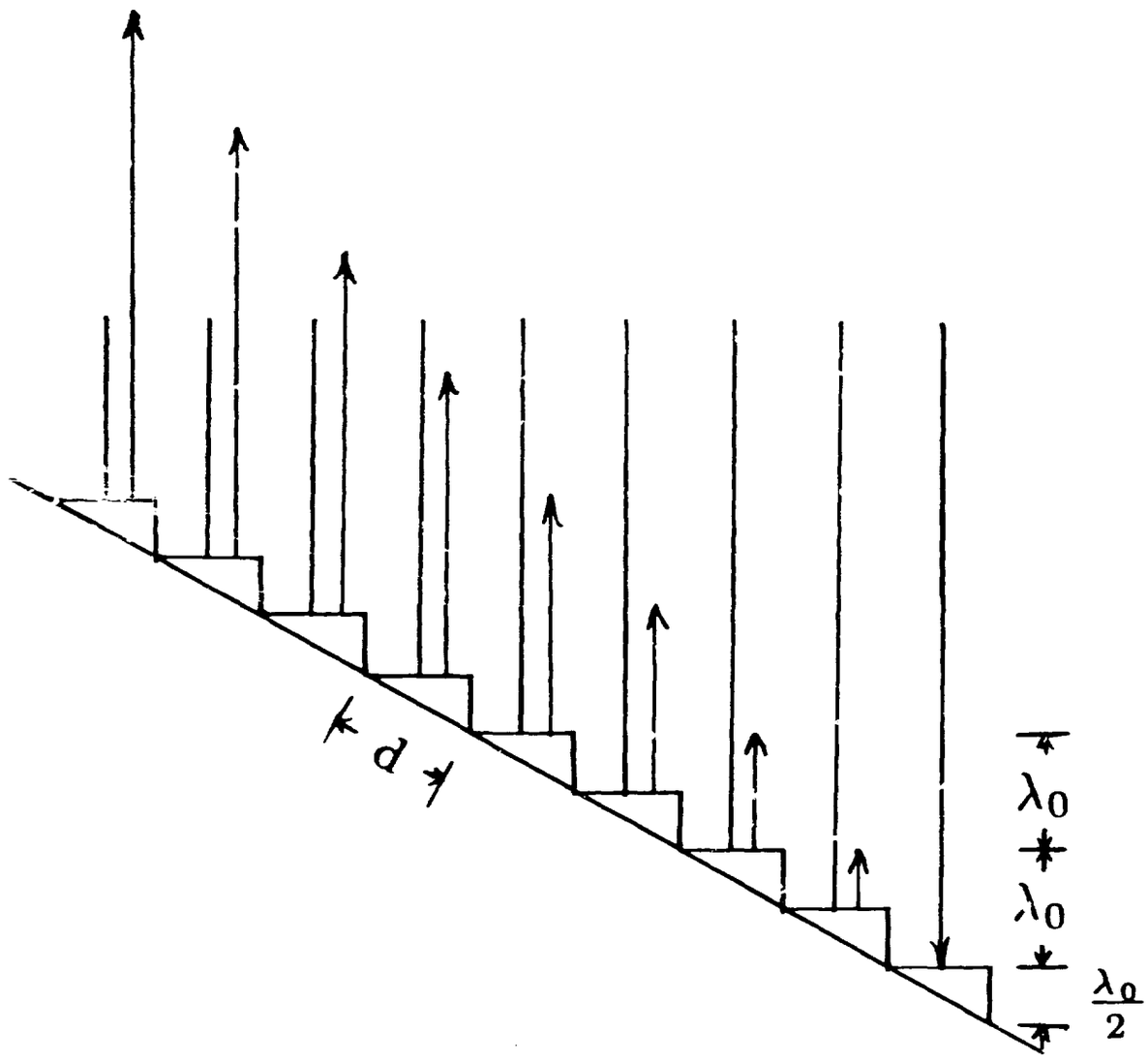
d
λ_0
λ_0
$\frac{\lambda_0}{2}$

Small Signal Gain

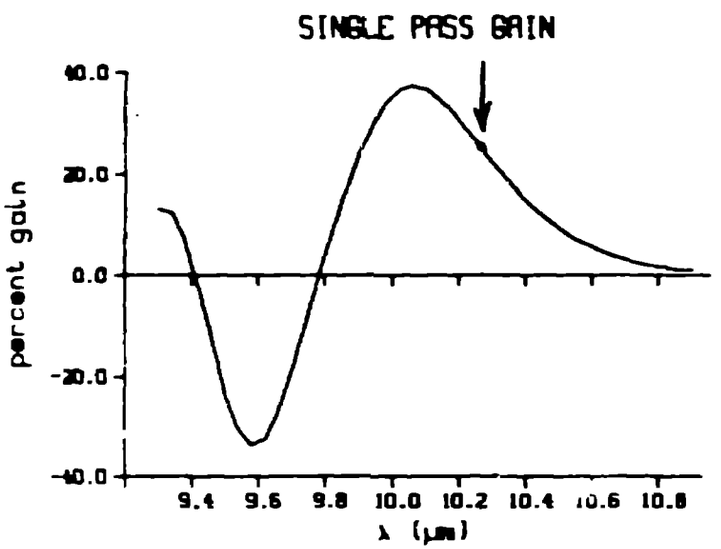

optical power density (w/cm^2) = 2.00×10^3

Large Signal Gain

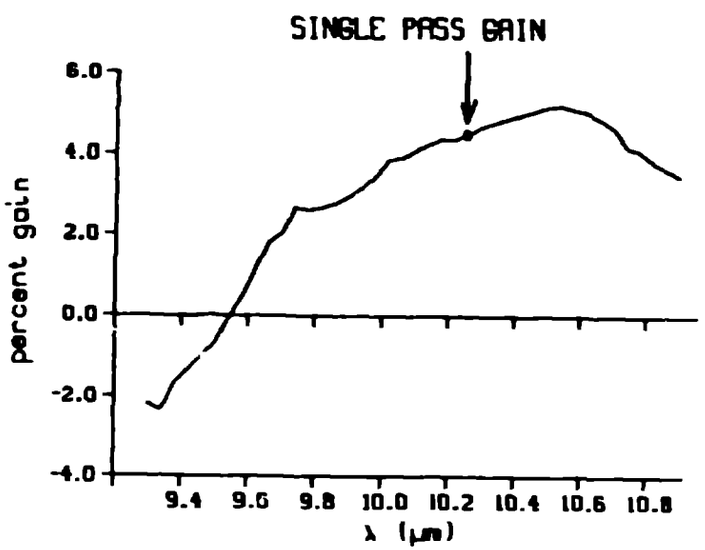

optical power density (w/cm^2) = 1.70×10^{11}

Typical
Small-Signal
↑
Large-Signal
↑
* Low-Pass Filter

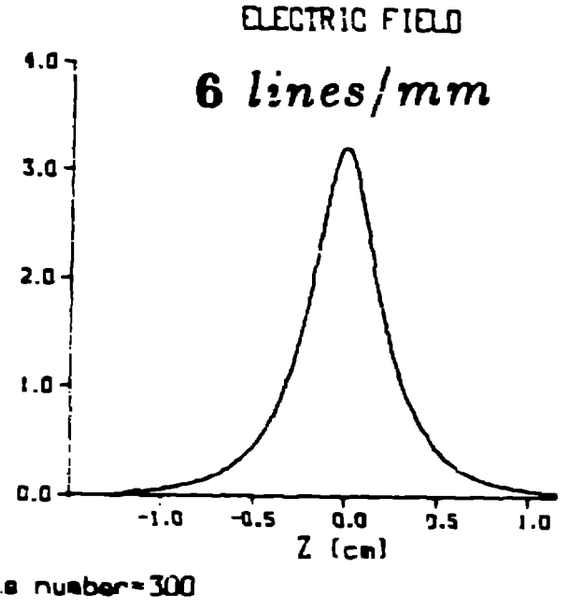

s number=300

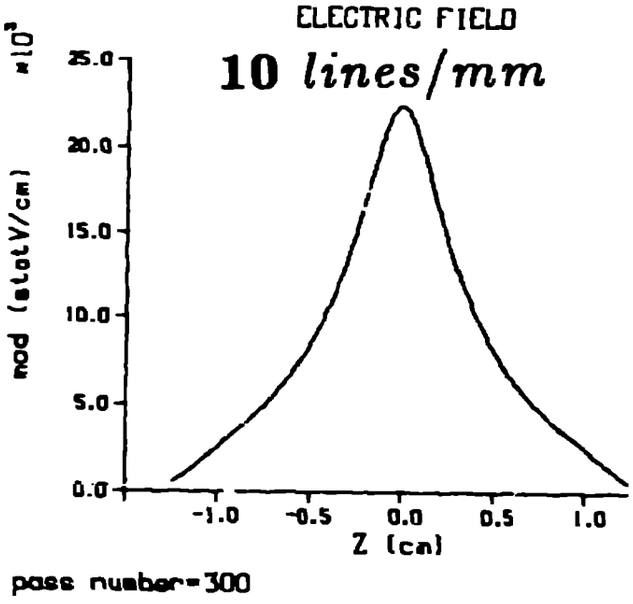

pass number=300

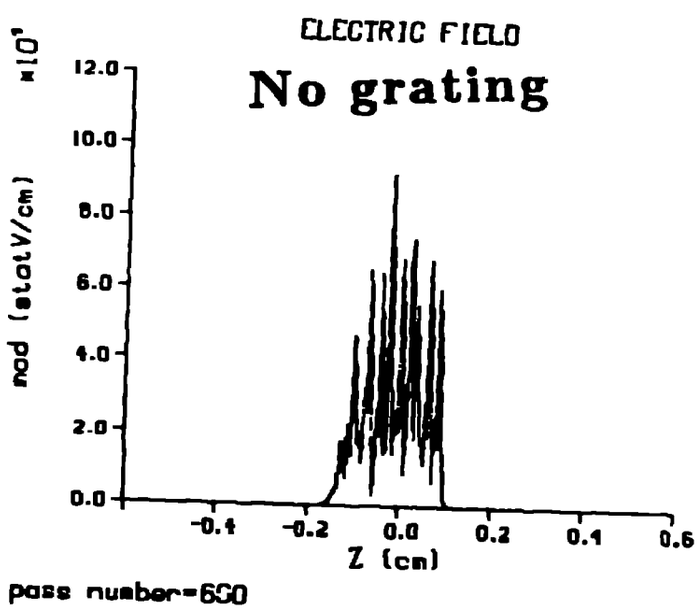

pass number=600

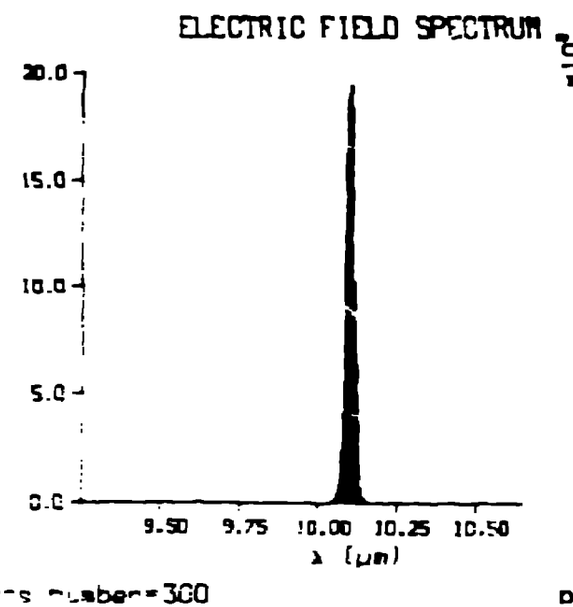

ss number=300

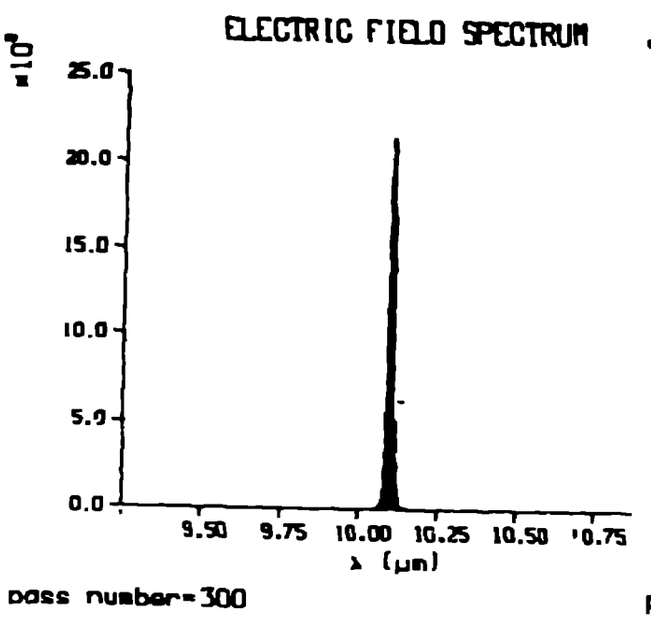

pass number=300

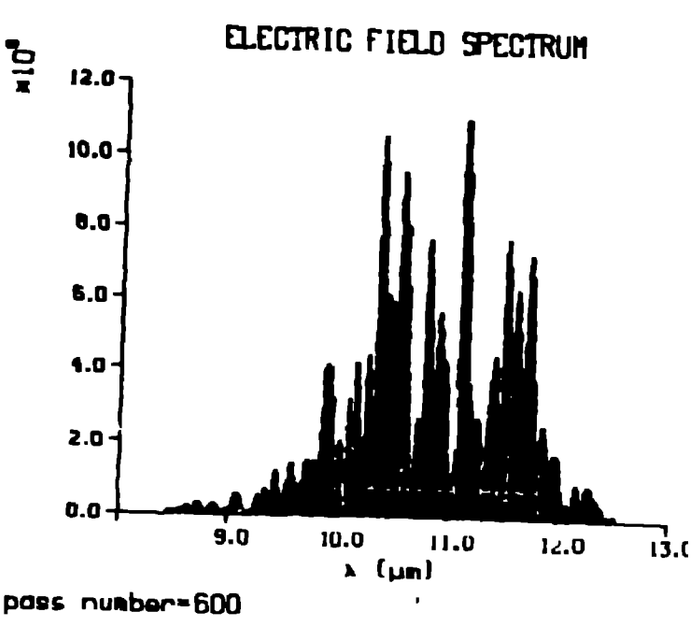

pass number=600

- **6 *lines/mm***

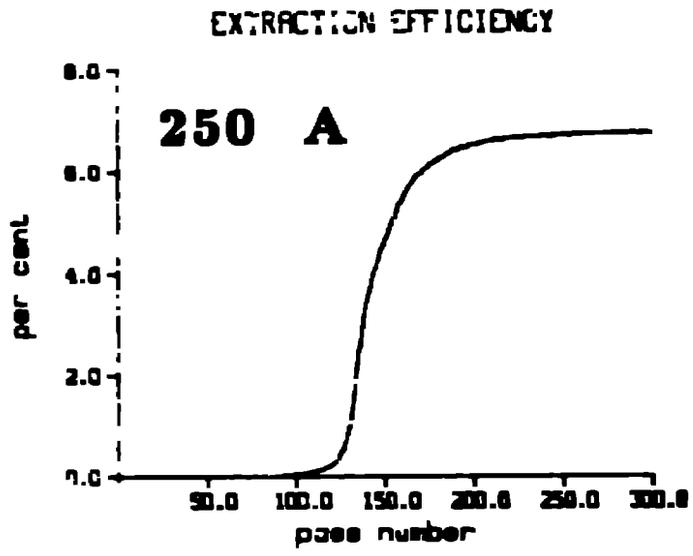

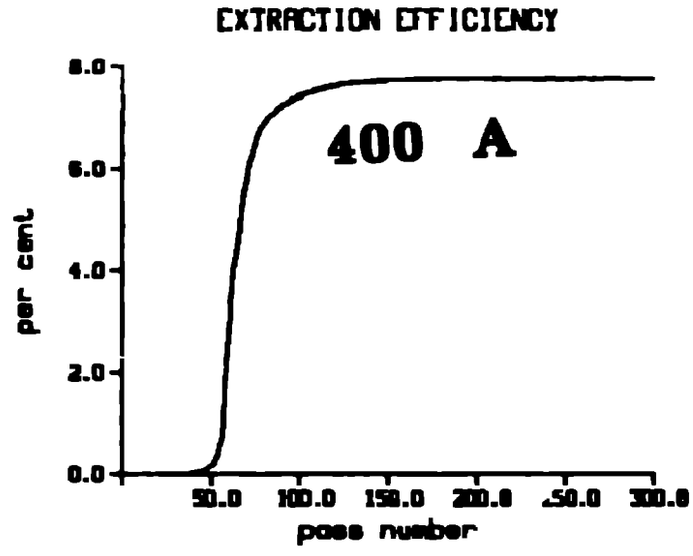

(c)

- **10 *lines/mm***

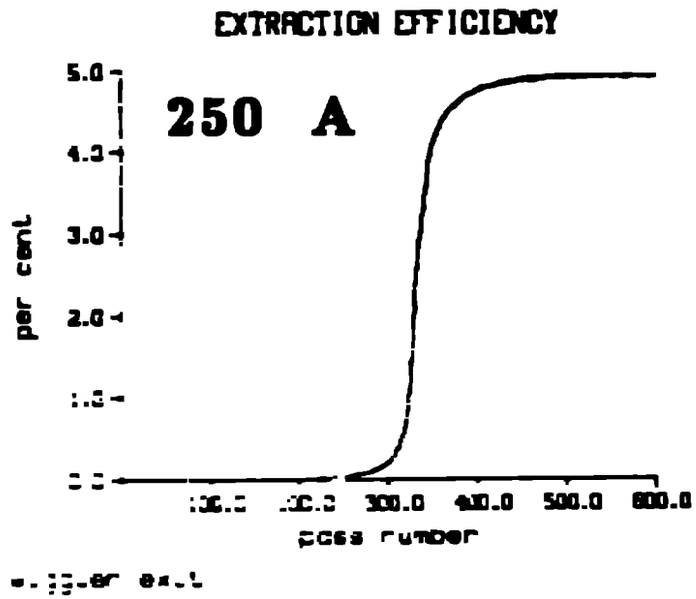

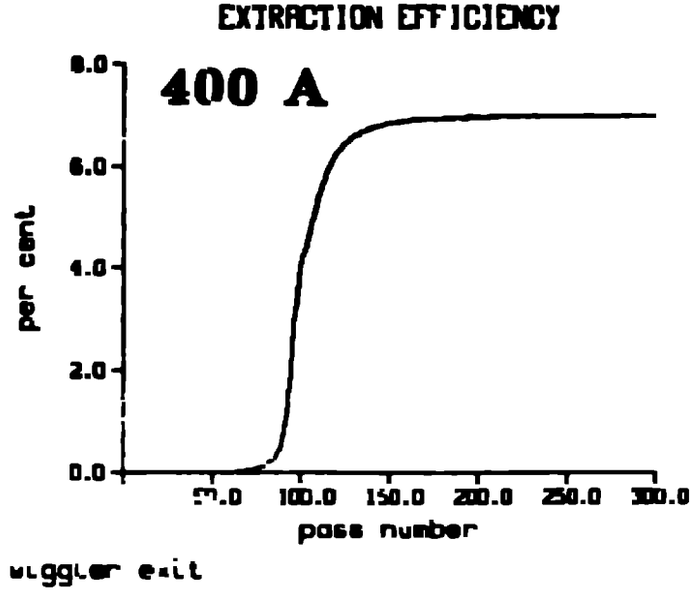

(b)

• No grating

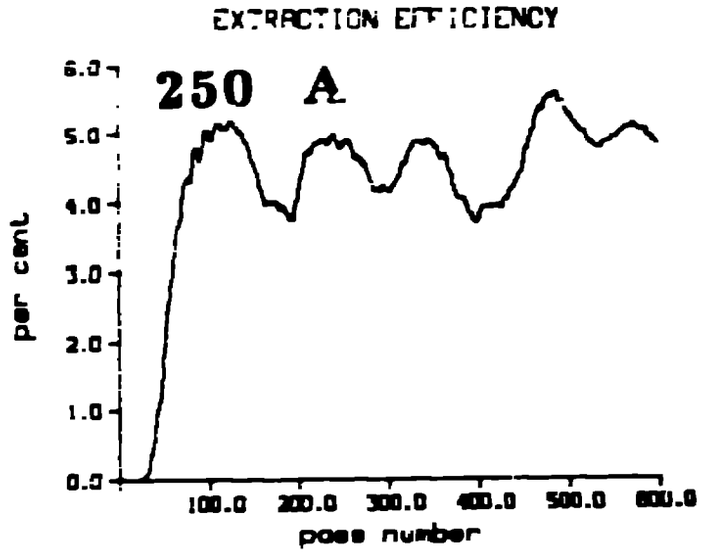

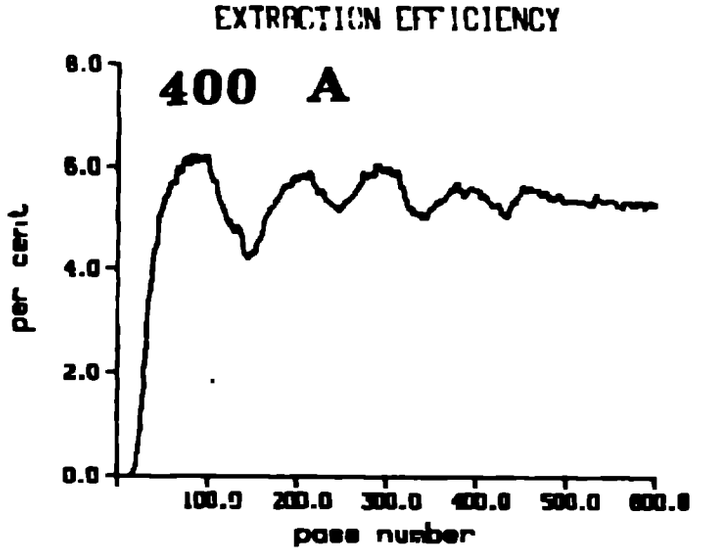

(a)

• Single Pass

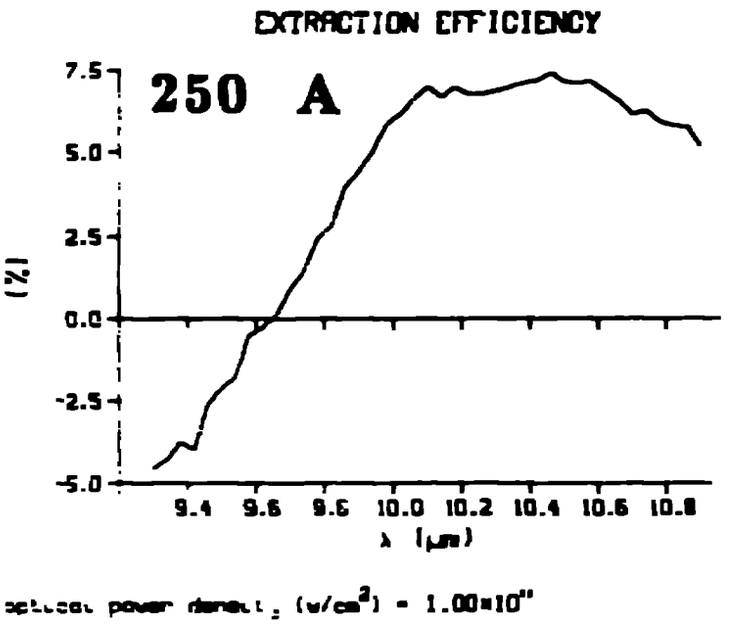

optical power density (w/cm²) = 1.00×10¹¹

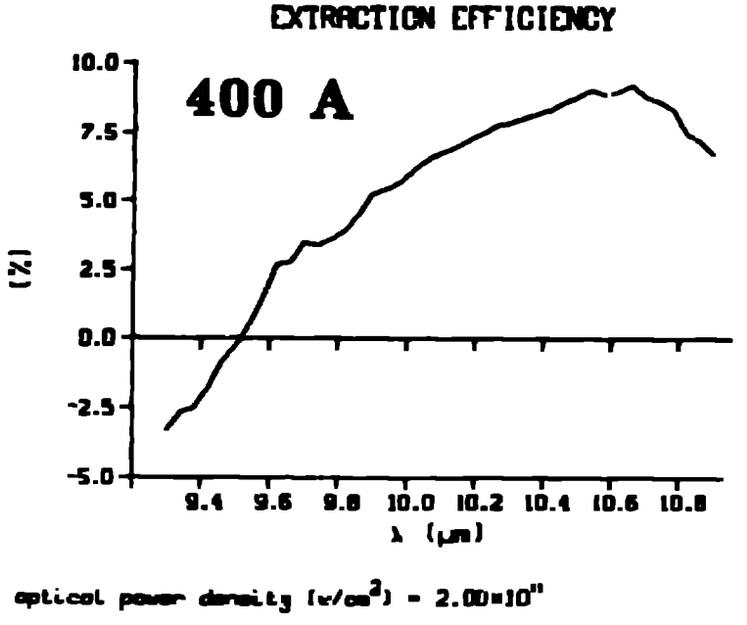

optical power density (w/cm²) = 2.00×10¹¹

(b)

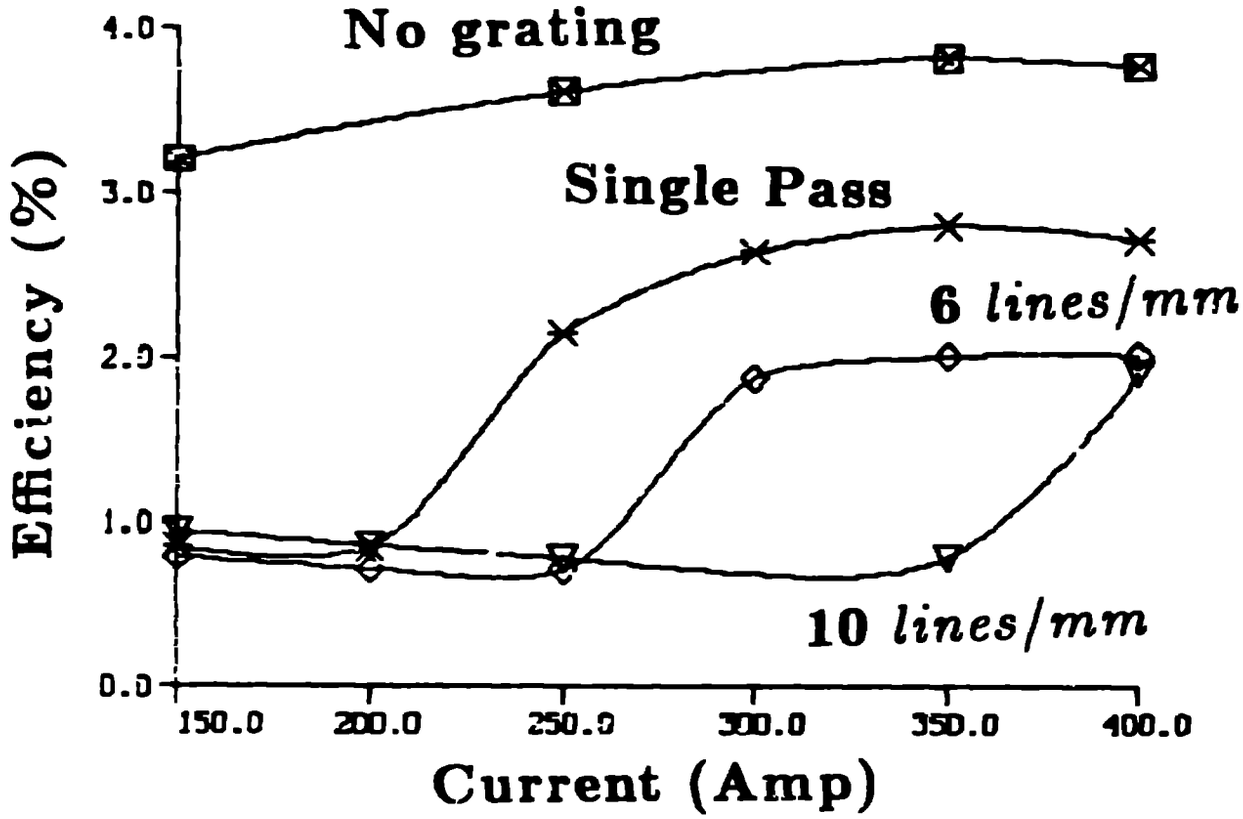
No grating
Single Pass
6 lines/mm
10 lines/mm
Efficiency (%)
4.0
3.0
2.0
1.0
0.0
150.0
200.0
250.0
300.0
350.0
400.0
Current (Amp)

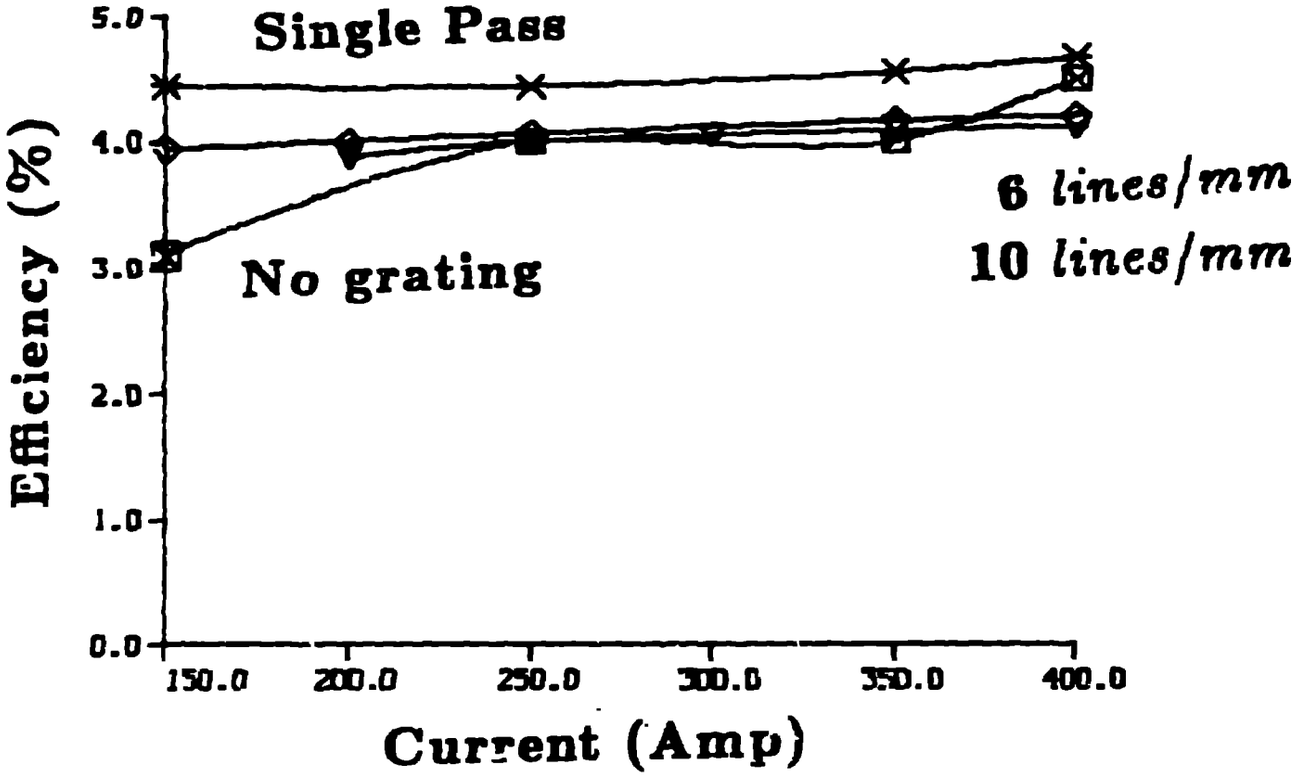
Single Pass
No grating
6 lines/mm
10 lines/mm
Efficiency (%)
5.0
4.0
3.0
2.0
1.0
0.0
150.0
200.0
250.0
300.0
350.0
400.0
Current (Amp)

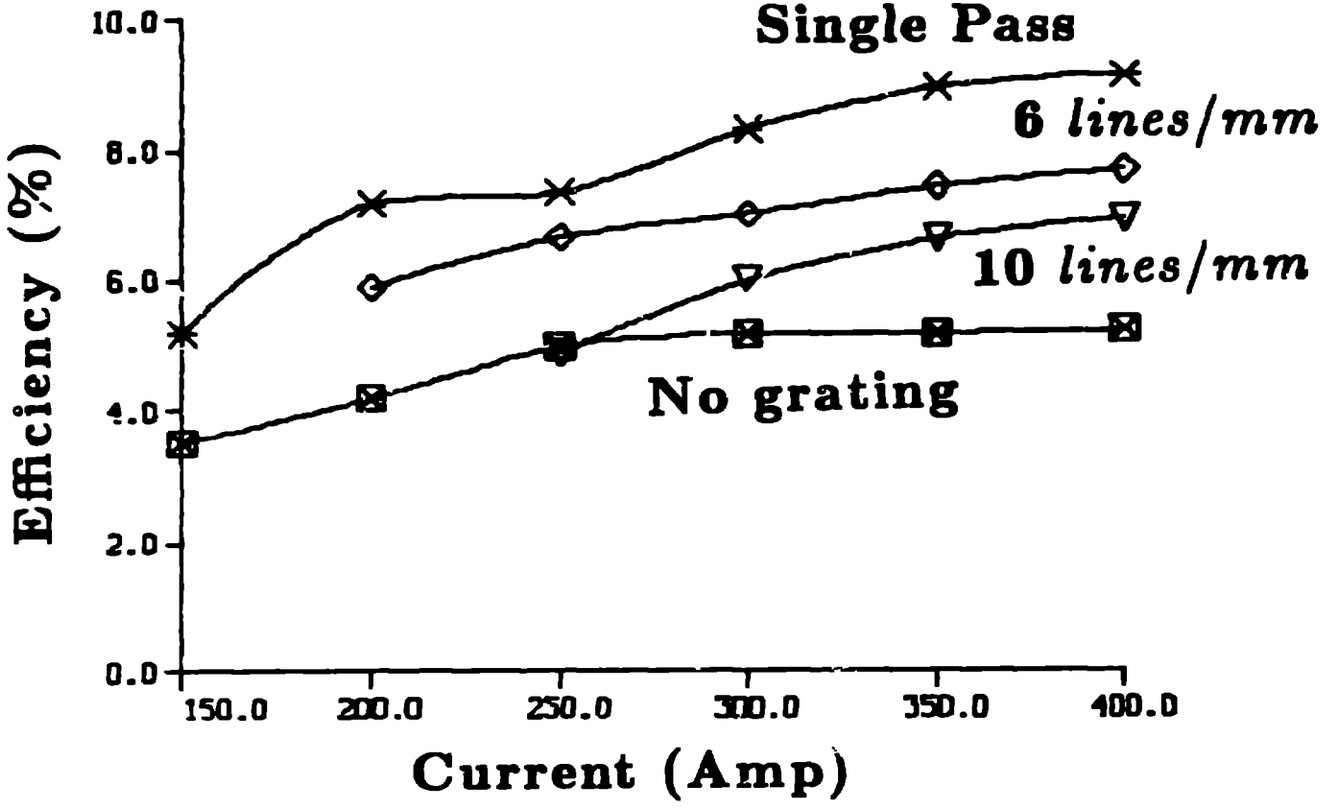
Single Pass
6 lines/mm
10 lines/mm
No grating
Efficiency (%)
10.0
8.0
6.0
4.0
2.0
0.0
150.0
200.0
250.0
300.0
350.0
400.0
Current (Amp)